Research Article | Submit Manuscript

Turkish Journal of Electromechanics & Energy

ISSN-2547-975X

Control of Fuel Cells-Electric Vehicle Based on Direct Torque Control

Z. Mokrani[1], D. Rekioua[1,*], T. Rekioua[1]

[1]Laboratoire LTII, Faculté de Technologie, Université de Bejaia, 06000 Bejaia, Algeria

Received: 4 April 2018; Revised: 6 September 2018; Accepted: 10 October 2018; Published: 1 December 2018

Turk J Electrom Energ Vol.: 3 No: 2 Page: 8-14 (2018)

SLOI: http://www.sloi.org/

*Correspondance E-mail: dja_rekioua@yahoo.fr

ABSTRACT In this paper, proton exchange membrane (PEM) fuel cell electric vehicle is presented as a solution to overcome the alarming pollution problems caused by the conventional internal combustion engine vehicles. To improve the performances of the electric vehicle, the direct torque control (DTC) is applied to the induction machine. It allows us to obtain higher performances with an increasing dependency of the electrical parameters. The use of the PEM fuel cells and the introduction of advanced controls to the DTC results in improved performance of the electric vehicle. The modeling of the whole system is also provided. Obtained results under MATLAB/Simulink was used the compute the performance values of the electric vehicle.

Keywords: Fuel Cell, Electric Vehicle, DTC, Induction Machine

Cite this article: Z. Mokrani, D. Rekioua, T. Rekioua, Control of Fuel Cells-Electric Vehicle Based on Direct Torque Control, Turkish Journal of Electromechanics & Energy, 3(2), 8-14, (2018).

1. INTRODUCTION

Currently, most of the world's energy production comes from fossil energy sources (oil, gas, coal etc.). Excessive consumption of these energy resources, leads to the depletion of these reserves and intensifies the release of greenhouse gases (CO_2, CH_4, etc.) which cause the pollution of the atmosphere. With these alarming consequences, it is necessary to consider the development of alternative energies. Renewable energy sources (wind, solar, biomass, geothermal, hydro etc.) and fuel cell technology are sustainable resources, offering a competitive ecological quality in terms of cost compared to conventional energy sources [1].

The PEM fuel cell is considered as a chemical renewable energy source since it uses H_2 and O_2, which are two abundant chemical elements, to produce energy. A proton exchange membrane fuel cell transforms the chemical energy liberated during the electrochemical reaction of hydrogen and oxygen to electrical energy, as opposed to the direct combustion of hydrogen and oxygen gases to produce thermal energy. The name of chemical source was given due to the reaction which occurs between O_2 and H_2. Output of the reaction is electrical energy, and water.

During the past few years, the fuel cell electric vehicle (EV) gained the interest of industrials, where it is presented as a clean mean of transportation, with no harmful emissions and noise. The development of fuel cell technology offers significant autonomy for the electric vehicle going up to 400-800 km. Most mobile applications and particularly automobiles are dominated by proton exchange membrane fuel cells (PEMFC) [2]. The advantages of the fuel cell allow us to exploit it in the electric vehicle, such as: higher efficiency; silent operation compared to internal combustion engines.

In this context, several studies present the drive of the EV with the fuel cell. Authors studied the electric fuel cell application, the generation of the hydrogen and the integration to the smart city [3-4]. However the control strategy of the electric machine is not addressed. Different types of machines have been used to move EVs. Due to the robustness and low-cost, Induction Motors (IM) have obtained special interests from the industry since their invention. This development allows the introduction of the advanced control, such as Direct Torque Control (DTC), Fuzzy Logic Control (FLC) and Sliding Mode Control (SMC), which are applied to the IMs in order to improve their performances [5-26]. Several researchers employed DTC as reported in literature [5-9, 13-20, 24-25]. In another study, authors used PI and Fuzzy Controller to control induction motor speed [21]. In order to improve performances, some authors have used a combination of several controllers. A combination of DTC and FLC was proposed for IM in [22-23, 26].

In this study, performances analyses of a PEM fuel cells electric vehicle using direct torque control (DTC) are presented. The use of this control method allows us to obtain better performances with an increasing dependency of the electrical parameters. The simulation has been carried out using MATLAB/Simulink.

2. MODELING OF THE PROPOSED SYSTEM

The proposed system is given in Figure 1. It consists principally of an electric vehicle supplied by proton exchange membrane fuel cells (PEMFC) and controlled by DTC control method. Each subsystem has been modeled separately. The electric vehicle has been modeled by an induction motor (IM) fed by an inverter. The global system has been simulated in MATLAB/Simulink.

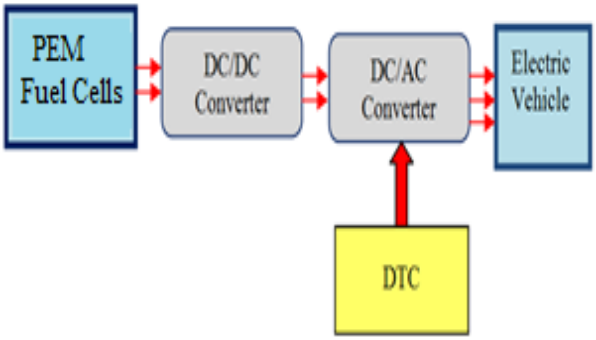

Fig. 1. Proposed PEM fuel cell model

2.1. PEM Fuel Cell Model

A PEMFC is an electrochemical energy converter. The cell voltage V_{PEMFC} is given as the summation of Nernst voltage E_{Nernst} due to various irreversible loss mechanisms, activation overvoltage V_{act}, concentration or diffusion over-voltage V_{conc} and resistive or ohmic over-voltage V_{ohm} as shown in Figure 2 [2, 5, 10, 11].

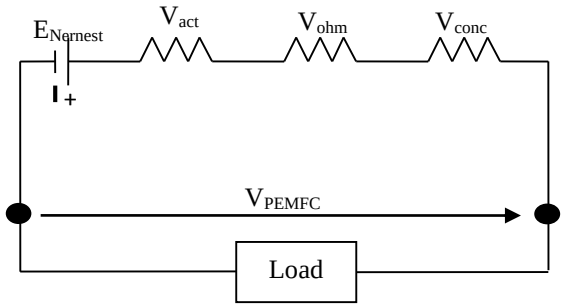

Fig. 2. Electrical representation of a PEMFC

$$V_{PEMFC} = E_{Nernest} - V_{act} - V_{ohm} - V_{conc} \quad (1)$$

$$E_{Nernest} = \alpha_1 + \alpha_2 \times (T_{PEMFC} - 298.15) + \alpha_3 \times T_{PEMFC} \left(0.5 \ln P^*_{O_2} + \ln P^*_{H_2}\right) \quad (2)$$

$$V_{act} = \beta_1 + \beta_2 \times T_{PEMFC} + \beta_3 \times T_{PEMFC} \times \ln\left(j \times 5 \times 10^{-3}\right) + \beta_4 \times T_{PEMFC} \times \ln C^*_{O2} \quad (3)$$

$$V_{ohm} = I_{PEMFC} (R_m + R_c) \quad (4)$$

and

$$R_m = \frac{r_m \times e_m}{S_{cell}} \quad (5)$$

$$V_{conc} = -B \times \ln\left(1 - \frac{j}{j_{max}}\right) \quad (6)$$

where V_{act} is activation overvoltage, V_{conc} is concentration or diffusion over-voltage, V_{ohm} is resistive or ohmic over-voltage, V_{PEMFC} is fuel cell voltage, $E_{Nernest}$ is Nernest voltage, α_i and β_I constants, T_{PEMFC} absolute operating temperature of the stack, P^*_{O2} partial oxygen pressures, P^*_{H2} partial hydrogen pressures, C^*_{O2} oxygen concentration in the cathode area, I_{PEMFC} fuel cell current, j current density, β constant, R_m equivalent resistance of the electron flow, R_c proton resistance, r_m specific resistance of the membrane, e_m thickness of the membrane, S_{cell} membrane active area, λ adjustable parameter in Equation 1 to 6.

Electrical characteristics of PEM fuel cells are represented in Figure 3 and the parameters of the fuel cell used in Equation 2 and 4 are summarized in Table 1.

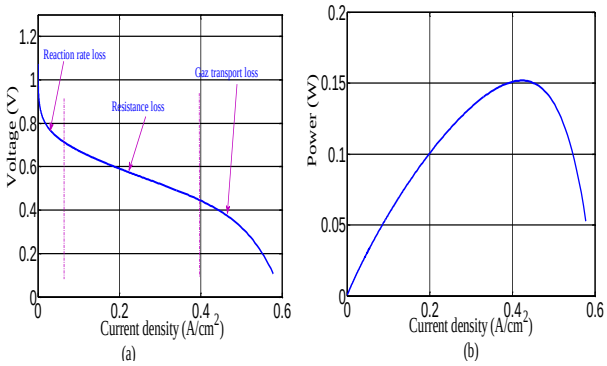

Fig. 3. Voltage characteristic (a), and power characteristic (b)

Table 1. Parameters of the fuel cell

Coefficients	Values
α_1	1.229
α_2	-8.5×10^{-4}
α_3	4.3085×10^{-5}
β_1	-0.9514
β_2	3.12×10^{-3}
β_3	-1.87×10^{-4}
β_4	7.4×10^{-5}

2.2. DC/DC Converter Model

The DC/DC boost converter used is inserted between the source and the inverter. The following equation gives voltage and current expressions of the DC/DC converter [2].

$$\begin{cases} V_{DC} = \dfrac{1}{1-D} V_{FC} \\ I_{DC} = (1-D) I_{FC} \end{cases} \quad (7)$$

2.3. Induction Motor Model

The stator voltage equations can be represented in a stationary reference frame as [1-2, 5, 9]:

$$\begin{cases} V_{s\alpha} = R_{s\alpha} i_{s\alpha} + \dfrac{d\Phi_{s\alpha}}{dt} \\ V_{s\beta} = R_{s\beta} i_{s\beta} + \dfrac{d\Phi_{s\beta}}{dt} \\ V_{r\alpha} = 0 = R_r i_{r\alpha} + \dfrac{d\Phi_{r\alpha}}{dt} - \omega_r \Phi_{r\beta} \\ V_{r\beta} = 0 = R_r i_{r\beta} + \dfrac{d\Phi_{r\beta}}{dt} - \omega_r \Phi_{r\alpha} \end{cases} \quad (8)$$

Equation (9) gives the electromagnetic torque and rotor speed equation:

$$\Gamma_e = \frac{3P}{2}\left(\Phi_{s\alpha} i_{s\beta} - \Phi_{s\beta} i_{s\alpha}\right)$$

$$J \frac{d\Omega}{dt} = \Gamma_e - \Gamma_r \quad (9)$$

Other parameters are listed in Table 2.

Table 2. Parameters of the induction machine

Parameters	*Symbols*	*Values*	*Units*
Shaft power	P_u	3	kW
Nominal speed	N_r	1430	rpm
Frequency	f	50	Hz
Number of pole pairs	P	2	-
Stator resistance	R_s	1.76	Ω
Rotor resistance	R_r	1.95	Ω
Mutual inductance	M	0.183	H
Stator (rotor) self-inductance	L_s=L_r	0.194	H
Moment of Inertia	J	0.02	kg.m^2
Coefficient of viscous friction	f	0.0001	N.m.s/rad

2.4. Methods for Identifying Induction Machine Parameters

Several methods exist to identify machine parameters (such as stator and rotor resistors, stator and rotor cyclic inductances and mutual inductance). We can cite:

- Least squares method (knowledge of partial leakage equivalent scheme and parameter vector).
- Nameplate method, which is a direct method (knowledge of the rated power factor and the model of the machine at steady speed).
- Conventional test method, which is based on the steady-state machine model used in our study.

The steady state phase scheme, also known as coupled inductance scheme, is as shown in Figure 4.

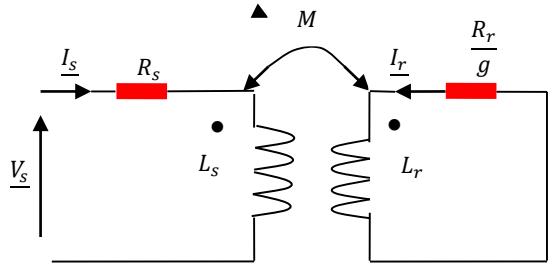

Fig. 4. Steady state phase diagram

$$\underline{V_s} = R_s\underline{I_s} + jL_s\omega_s\underline{I_s} + jM\omega_s\underline{I_r}$$
$$0 = \frac{R_r}{g}\underline{I_r} + jL_r\omega_s\underline{I_s} + jM\omega_s\underline{I_s} \quad (10)$$

We performed the continuous test on one phase to determine the stator resistance R_s of the machine since the inductance term is zero.

The test in synchronism at no load allows us to annul the slip "g'", and we will have as equivalent model of the machine as shown in Figure 5.

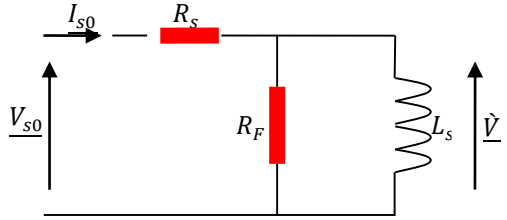

Fig. 5. The equivalent diagram of the machine under synchronism test

No need for these power active P_0 , reactive power $Q_0 = \sqrt{S_0^2 + P_0^2}$, the efficace current I_{so}, the voltage efficace V_{so}.

$$P_0 = R_s \cdot I_{so}^2 + \frac{\grave{V}^2}{R_F} \quad (11)$$
$$Q_o = \frac{\grave{V}^2}{L_s \cdot \omega} \quad (12)$$
$$\grave{V} = V_{so} \cdot \frac{R_F \cdot L_s \cdot \omega_s}{\sqrt{(R_s \cdot R_F)^2 + (L_s \cdot \omega_s \cdot (R_F + R_s))^2}} \quad (13)$$

The current I_{so} is very low in this test and the voltage losses due to the stator resistance are generally neglected before the voltage V_{so}, so from the previous equations we will have the following equations:

$$P_0 = \frac{V_{so}^2}{R_F} \quad (14)$$
$$Q_o = \frac{V_{so}^2}{L_s \cdot \omega_s} \quad (15)$$

Since the studied machine is a Squirrel-cage Class A (assumption of equal leakage distribution in the stator and rotor), therefore: $L_s = L_r$ [27-28].

During locked rotor and reduced voltage test (short circuit), the rotor is locked, so the speed is zero, which will imply that the slip is at its maximum value (g=1). The equivalent model of the machine is given in Figure 6.

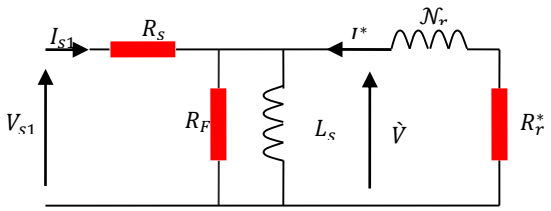

Fig. 6. Equivalent diagram of the locked rotor test machine

We have:

$$P_1 = R_s \cdot I_{s1}^2 + \grave{V}^2 \cdot \left(\frac{1}{R_F} + \frac{R_r^*}{(\mathcal{N}_r \cdot \omega_s)^2 + R_r^{*2}}\right) \quad (16)$$
$$Q_1 = \grave{V}^2 \cdot \left(\frac{1}{L_s \cdot \omega_s} + \frac{R_r^*}{(\mathcal{N}_r \cdot \omega_s)^2 + R_r^{*2}}\right) \quad (17)$$
$$\grave{V} = V_{s1} - R_s \cdot I_{s1} \quad (18)$$
$$\mathcal{N}_r = L_s \cdot \left(\frac{L_s^2}{M^2} - 1\right) \quad (19)$$
$$R_r^* = R_r \cdot \frac{L_s^2}{M^2} \quad (20)$$

As the voltage V_{s1} is low, it is possible to neglect the currents flowing in R_F and L_s before I_{s1} and the previous equations become :

$$P_1 = (R_s + R_r^*) \cdot I_{s1}^2 \quad (21)$$
$$Q_1 = \mathcal{N}_r \cdot \omega_s \cdot I_{s1}^2 \quad (22)$$

2.4. Electric Vehicle Model

The vehicle is subjected to forces along the longitudinal axis. There are types of three forces [1-2, 5]: -Rolling resistance force F_{tire} due to the friction of the vehicle tires on the road. It is given as:

$$F_{tire} = m \times g \times f_{ro} \quad (23)$$

With: m is the vehicle total mass, g is the gravity acceleration, fro is the rolling resistance force constant.
- Aerodynamic drag force F_{aero} caused by the friction on the body moving through the air. Its expression is:

$$F_{aero} = (1/2) \times \rho_{air} \times A_f \times C_d \times V^2 \quad (24)$$

With: ρ_{air} is the air density, A_f is the frontal surface area of the vehicle, C_d is the aerodynamic drag coefficient, V is the vehicle speed.

-Climbing force F_{slope} which depends on the road slope.

$$F_{slope} = m \times g \times sin(\beta) \quad (25)$$

With: β is the road slope angle.

The total resistive force F_r is given as:

$$F_r = F_{tire} + F_{aero} + F_{slope} \quad (26)$$

The load torque can be written as:

$$T_r = F_r \times \frac{r}{G} \quad (27)$$

where r is the tire radius, F_r is the total force.

By applying the fundamental principle of the vehicle dynamics, we can deduce the speed vehicle.

$$m\frac{dv}{dt} = F_t - F_r \quad (28)$$

where F_t is traction force. Table 3 summarizes the electric vehicle parameters.

Table 3. Parameters of the electric vehicle

Parameters	Symbol	Value	Unit
Vehicle total mass	m	1300	kg
Rolling resistance force constant	f_{ro}	0.01	
Air density	ρ_{air}	1.20	kg/m^3
Frontal surface area of the vehicle	A_f	2.6	m^2
Tire radius	r	0.25	m
Aerodynamic drag coefficient	C_d	0.32	
Gear speed ratio	G	5	
Road angle slope	β	60	°

3. DIRECT TORQUE CONTROL STRATEGY

To keep the DC bus voltage at a constant value when the speed of the rotor varies, different control techniques can be used. In our work, the IM is controlled using DTC strategy, which is a powerful control method for motor drives. The DTC technique is based on the independently control of the stator flux and electromagnetic torque.

For this purpose, the selection of the optimal space vector using a hysteresis controller is required. Similarly, the stator flux, electromagnetic torque developed by the machine and its position in terms of flux can be estimated [1-2].

Stator flux and electromagnetic torque are estimated using the following equations:

$$\begin{cases} \Phi_{s\alpha}(t) = \int_0^t (V_{s\alpha} - R_s * i_{s\alpha})dt \\ \Phi_{s\beta}(t) = \int_0^t (V_{s\beta} - R_s * i_{s\beta})dt \end{cases} \quad (29)$$

$$\Phi_s = \sqrt{\Phi_{s\alpha}^2 + \Phi_{s\beta}^2} \quad (30)$$

$$\theta_s = arctan\left(\frac{\Phi_{s\beta}}{\Phi_{s\alpha}}\right) \quad (31)$$

The electromagnetic torque is calculated using Equation 32.

$$\Gamma_e = \frac{3P}{2}\left(\Phi_{s\beta} i_{s\alpha} - \Phi_{s\alpha} i_{s\beta}\right) \quad (32)$$

The evolution of the stator flux in (αβ) frame is divided into six zones i, with i =[1: 6] as seen in Figure 7. The space vector applied in each condition is described in Table 4 [4-5].

Table 4. Switching table for the DTC technique

	N	1	2	3	4	5	6
H_Φ=1	H_Γ = 1	110	010	011	001	101	100
	H_Γ = 0	111	000	111	000	011	001
	H_Γ =-1	101	100	110	010	011	001
H_Φ=0	H_Γ = 1	010	010	011	001	101	100
	H_Γ = 0	000	000	111	000	111	000
	H_Γ =-1	001	001	101	100	110	010

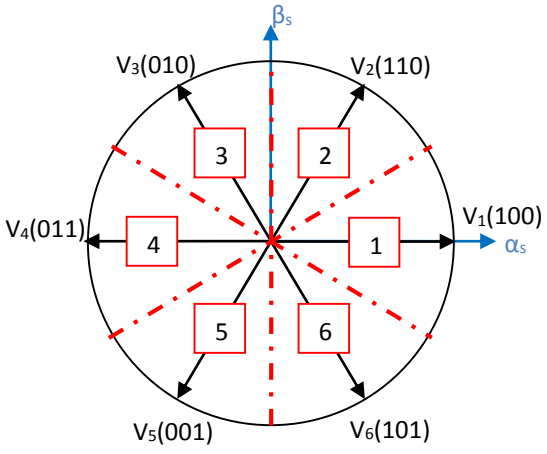

Fig. 7. The six voltage vector of the inverter

4. SIMULATION RESULTS AND DISCUSSION

MATLAB/Simulink has been used in the development of the DTC of induction motor using the above equations. The general studied system is represented in Figure 8.

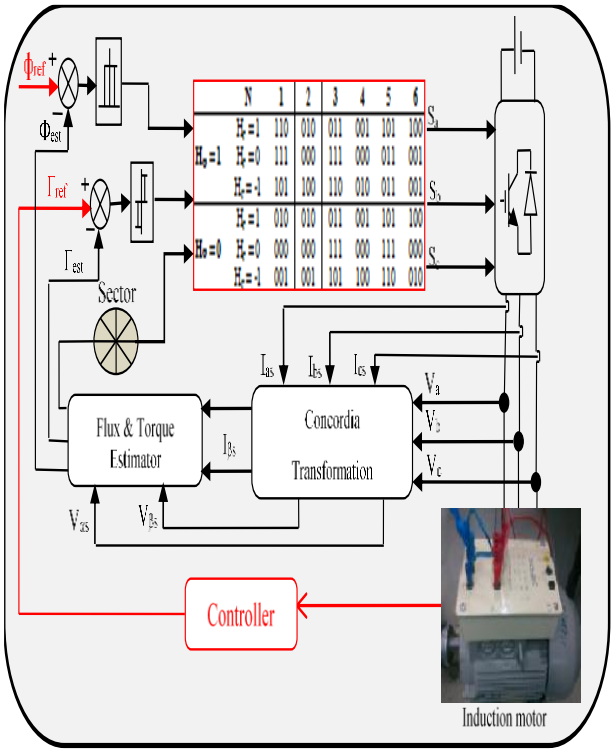

Fig. 8. General structure of the proposed direct torque control

The block diagram of the classical DTC is made under MATLAB/Simulink. The obtained results are given below. A vehicle speed profile is chosen to show the traction, the stop and the braking modes of the EV. The speed increases gradually from the moment t =9 s.

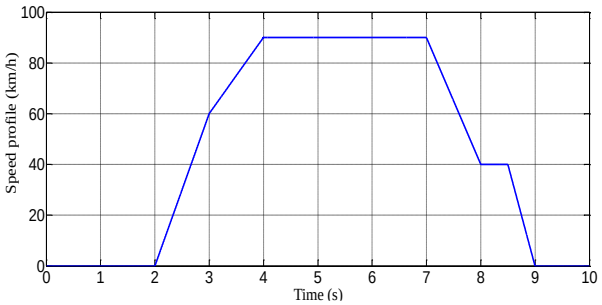

Fig. 9. Speed profile of the EV

The electromagnetic torque follows the load torque developed by the electric vehicle.

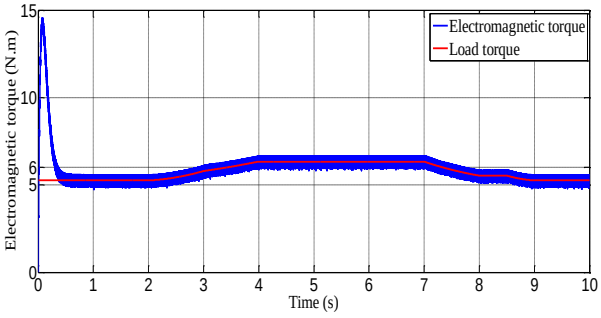

Fig. 10. Electromagnetic torque waveform

The biphase currents are in quadrature form (Figure 11) while the three-phase currents are shifted by $2\pi/3$ in Figure 12. The currents are alternative and reach a value of 5.6 A for a load torque of 6.3 N.m.

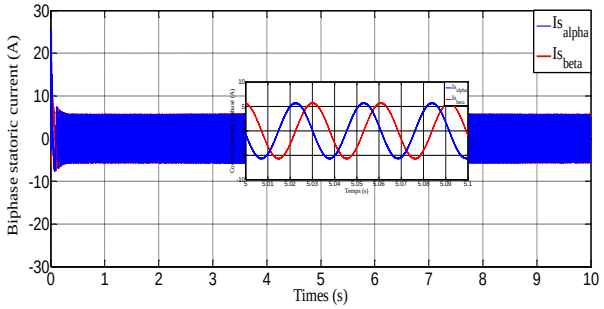

Fig.11. Biphase stator currents

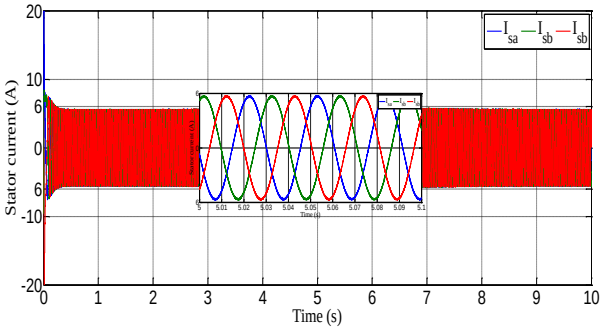

Fig. 12. Stator current waveform with classical DTC

The rotational speed of the induction is maintained to the reference imposed by the speed regulator (at 100 rad/s), despite the variation in the load applied to the electric machine. The direct and quadrature flux components are shifted by $\pi/2$ and have amplitude of 1Wb as shown in Figure 13. This amplitude is kept constant despite load torque variations.

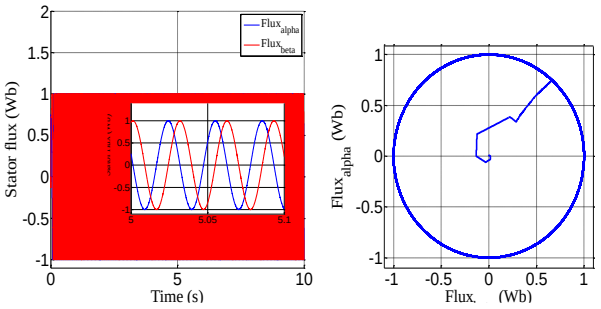

Fig. 13. Stator flux waveform and its circular trajectory

Although the DTC is insensitive to variations in the rotor parameters of the machine, the flow and torque estimation as well as the determination of the PI controller parameters are dependent on the stator resistance. This led us to the use of a controller ensuring total independence of the performances and accuracy of the technique with respect to the variation of the machine parameters.

6. CONCLUSION

An electric vehicle powered by the PEMFC is studied in this paper. The studied system deals the supply and the control of the electric vehicle using a sustainable energy and advanced control techniques. The obtained results show that the fuel cell insures the energy need of the EV. Firstly, a DTC method has been applied to control electric vehicle. Obtained results show the performances of the proposed system.

References

[1] F. Tazerart, Z. Mokrani, D. Rekioua, and T. Rekioua, Direct torque control implementation with losses minimization of induction motor for electric vehicle applications with high operating life of battery, Intern. Jour. of Hydrogen Energy, 39, 13827-38, (2015).

[2] Z. Mokrani, D. Rekioua, T. Rekioua, Modeling, Control and Power Management of Hybrid Photovoltaic Fuel Cells with Battery Bank Supplying Electric Vehicle, International Journal of Hydrogen Energy, 39(27), 15178-87, (2014).

[3] V. Oldenbroek, L. A Verhoef, and Ad. J. M. Van Wijk, Fuel cell electric vehicle as a power plant: Fully renewable integrated transport and energy system design and analysis for smart city areas, International Journal of Hydrogen Energy, 42(12), 8166-96, (2017).

[4] X. Lian, Wang, and J. Song, Fuel consumption optimization for smart hybrid electric vehicle during a car-following process, International Journal of Hydrogen Energy, 87, 17-29, (2017).

[5] D. Rekioua, E. Matagne, Optimization of photovoltaic power systems: Modelization, Simulation and Control, Green Energy and Technology, 102, (2012).

[6] N. Mebarki, T. Rekioua, Z. Mokrani, and D. Rekioua, Supervisor control for stand-alone photovoltaic/ hydrogen/ battery bank system to supply energy to an electric vehicle, International Journal of Hydrogen Energy, 39, 13777-88, (2015).

[7] S. G. Buja, Direct torque control of PWM inverter-Fed AC motor-a survey, IEEE Trans. Industrial Electronics, 4744-57, (2004).

[8] A. Haddoun, M. Benbouzid, D. Diallo, R. Abdessemed, J. Ghouili, and K. Srairi, A Loss-Minimization DTC Scheme for EV Induction Motor, IEEE Trans on Vehicular Technology, 56(1), 81-88, (2007).

[9] Z. Keliang, J.A. Ferreira , S.W.H. de Haan, Optimal energy management strategy and system sizing method for stand-alone photovoltaic-hydrogen systems, International Journal of Hydrogen Energy, 33(2), 477-489, (2008).

[10] D. Rekioua, S. Bensmail, N. Bettar, Study of hybrid photovoltaic/fuel cell system for stand-alone applications, International Journal of Hydrogen Energy, 39(3), 13820-26. (2014).

[11] Y. Liu , X. Wu, L. Huang, SVPWM method for performance improvement of direct torque control, Qinghua Daxue Xuebao/Journal of Tsinghua University, 44 (7), 869-872, (2004).

[12] N. Cui, C. Zhang, Z. Lu, K. Li, Fast torque response control of high efficiency drives in electric vehicles based on voltage space vector, Diangong Jishu Xuebao/Transactions of China Electrotechnical Society, 24(3) , 61-66, (2009).

[13] D. Rekioua, T. Rekioua, DSP-controlled direct torque control of induction machines based on modulated hysteresis control, Proceedings of the International Conference on Microelectronics, ICM, art. no. 5418603, 378-381, (2009).

[14] R. Abdelli, D. Rekioua, T. Rekioua, A. Tounzi. Improved direct torque control of an induction generator used in a wind conversion system connected to the grid; ISA Transactions, 52(4). 525-538, (2013).

[15] S. Jiangua, C. Quanshi. Research of Electric Vehicle IM Controller Based on Space Vector Modulation Direct Torque Control, Proceeding of the Eighth International Conference on Electric Machine and Systems ICEMS, vol. 2, 1617-20, (2005).

[16] R. Toufouti, S. Meziane, H. Benalla, Direct Torque Control for Induction Motor Using Fuzzy Logic, ACSE Journal, 6(2),19-26, (2006).

[17] H. Ehsan, A. K. Davood, DTC-SVM Scheme for Induction Motors Fed with a Three-level Inverter, World Academy of Science, Engineering and Technology, vol. 44, 168-172, (2008).

[18] S. M. Gadoue, D. Giaouris, J. W. Finch, Artificial Intelligence-Based Speed Control of DTC Induction Motor Drives- a Comparative Study, Electric Power System Research, 79, 210-19, (2009).

[19] J. Q. Yang, J. Huan, Direct Torque Control System for Induction Motors with Fuzzy Speed PI Regulator, IEEE Proceeding of the fourth International Conference on Machine Learning and Cybernetics, Guangzhou, vol. 2, 778-783, (2005).

[20] S. Gowrishankar, K. Kirshnamoorthi, Speed Control of Induction Motor Using PI and Fuzzy Controller, Journal of Innovative Research and Solution (JIRAS), 1A(2). 50-57, (2013).

[21] Y. Goa, J. Wang, X. Qiu, The Improvement of DTC System Performance on Fuzzy Control, 3rd International Conference on Environmental Science and Information Application Technology, vol. 10, 589-584, (2011).

[22] S. Tamalouzt, N. Benyahia, T. Rekioua, D. Rekioua, R. Abdessemed, Performances analysis of WT-DFIG with PV and fuel cell hybrid power sources system associated with hydrogen storage hybrid energy system, International Journal of Hydrogen Energy, 41(45), 21006-21, (2016).

[23] L. Yen-Shin, L. Juo-Chiun, New Hybrid Fuzzy Controller for Direct Torque Control Induction Motor Drives, IEEE Trans. Power Electronics , vol. 18, No. 5, 1211-19, (2003).

[24] S. Sharma, O. P. Jaga, and S. K. Maury, Modeling and Control Strategies for Energy Management System in Electric Vehicles, Perspectives in Science, vol. 8, 358-360, (2006).

[25] S. Taraft, D. Rekioua , D. Aouzellag , S. Bacha , A proposed strategy for power optimization of a wind energy conversion system connected to the grid Energy Conversion and Management, 101 , 489-502 (2015).

[26] F. Barrero, Gonzâlez, A. Torralba, E. Galvân, L. G Franquelo, Speed control of induction motor using fuzzy sliding-mode structure, IEEE Trans. Fuzzy Systems, 3375-83, (2004).

[27] J. J. Cathey, Electric Machines: Analysis and Design Applying Matlab, McGraw Hill, (2001).

[28] Z. Salleh, F. A. Patakor, A. N. A. Rashid, Study on parameter determination for 1.5kW AC induction motor, Conference: Seminar Penyelidikan Zon Utara 2013, At: Politeknik Tuanku Syed Sirajuddin, (2013).

Biographies

Zahra Mokrani received her master's degree in electrical engineering from the University of Bejaia, Algeria, in 2012. She is Ph.D. student in the same department since 2016. Her current research interests are electrical system and control.

E-mail address: mokrani-zahra@hotmail.fr

Djamila Rekioua obtained her engineering degree in electrical engineering in 1987, the master's degree, in 1993, both from National Polytechnic Institute of Algeria, and the Ph.D. degree in 2002. Her research interests include control of AC machines and electric drives, and renewable energies (photovoltaic, wind turbine, and hybrid systems). Since 1989, she is teaching and pursuing research; firstly at the University of Sciences and Technology, (Algeria) and now she is Professor at the University of Bejaia (Algeria), head of the Team Renewable Energy in LTII Laboratory of the University of Bejaia.

E-mail address: dja_rekioua@yahoo.fr

Toufik Rekioua received his engineering degree from the National Polytechnic Institute of Algeria and earned the Doctoral degree from I.N.P.L of Nancy (France) in 1991.
He is Professor at the Electrical Engineering Department-University of Bejaia (Algeria) since 1992. He is presently the director of the LTII laboratory. His research activities have been devoted to several topics: control of electrical drives, modelling, wind turbine and control in AC machines.

E-mail address: to_reki@yahoo.fr